Article

Synthesis of New [8Fe-7S] Clusters: A Topological Link between the Core Structures of P-Cluster, FeMo-co, and FeFe-co of Nitrogenases

Yasuhiro Ohki, Yohei Ikagawa, and Kazuyuki Tatsumi

J. Am. Chem. Soc., **2007**, 129 (34), 10457-10465• DOI: 10.1021/ja072256b • Publication Date (Web): 03 August 2007

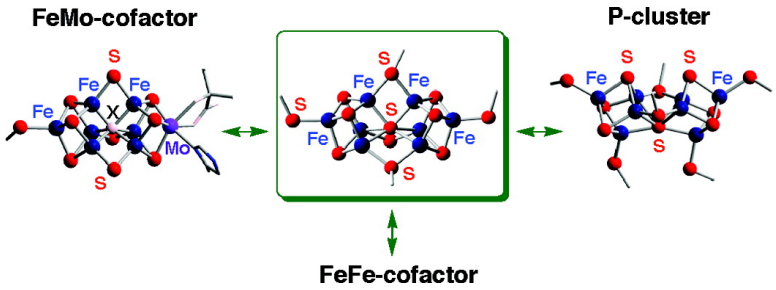

More About This Article

Additional resources and features associated with this article are available within the HTML version:

- Supporting Information
- Links to the 12 articles that cite this article, as of the time of this article download
- Access to high resolution figures
- Links to articles and content related to this article
- Copyright permission to reproduce figures and/or text from this article

View the Full Text HTML

J|A|C|S
ARTICLES
Published on Web 08/03/2007

Synthesis of New [8Fe-7S] Clusters: A Topological Link between the Core Structures of P-Cluster, FeMo-co, and FeFe-co of Nitrogenases

Yasuhiro Ohki, Yohei Ikagawa, and Kazuyuki Tatsumi*

Contribution from the Department of Chemistry, Graduate School of Science, and Research Center for Materials Science, Nagoya University, Furo-cho, Chikusa-ku, Nagoya 464-8602, Japan

Received March 31, 2007; E-mail: i45100a@nucc.cc.nagoya-u.ac.jp

Abstract: A coordinatively unsaturated dinuclear iron(II) complex of bulky thiolates, $[(TipS)Fe(\mu\text{-}SDmp)]_2$ (**1**; Tip = 2,4,6-^{i}Pr$_3$C$_6$H$_2$, Dmp = 2,6-(mesityl)$_2$C$_6$H$_3$), was synthesized from stepwise reactions of $Fe\{N(SiMe_3)_2\}_2$ with 1 equiv of HSDmp and then with 1 equiv of HSTip. Complex **1** was found to react with elemental sulfur (S_8) in toluene to generate a new class of [8Fe-7S] cluster, $[(DmpS)Fe_4S_3]_2(\mu\text{-}SDmp)_2(\mu\text{-}STip)(\mu_6\text{-}S)$ (**2**). The cluster **2** was also produced from one-pot reactions of $Fe\{N(SiMe_3)_2\}_2$ + HSDmp + HSTip + S_8 (8:6:10:7/8) and $Fe_3\{N(SiMe_3)_2\}_2(\mu\text{-}STip)_4$ + HSDmp + S_8 (8/3:16/3:7/8), where another [8Fe-7S] cluster, $[(TipS)Fe_4S_3]_2(\mu\text{-}SDmp)_2\{\mu\text{-}N(SiMe_3)_2\}(\mu_6\text{-}S)$ (**3**), was also found as a minor byproduct. In either of the clusters, two Fe_4S_3 incomplete cubane units are connected by three anionic ligands, namely three thiolate S atoms for **2** or two thiolate S atoms and one amide N atom for **3**, and one hexa-coordinate S atom resides at the center of the [8Fe-7S] core. They have a common $Fe(II)_5Fe(III)_3$ oxidation states, and an $S = {}^1/_2$ ground spin state was indicated by rhombic EPR signals at 10 K with $g = 2.19$, 2.07, and 1.96 for **2** and $g = 2.13$, 2.06, and 1.93 for **3**. The structural relevance of clusters **2** and **3** to P-cluster, FeMo-co, and FeFe-co of nitrogenases is discussed.

Introduction

The MoFe-nitrogenase is unique among known metalloenzymes, in that the enzyme is capable of reducing dinitrogen to ammonia under mild conditions, and in that the active sites, namely P-cluster and FeMo-cofactor, consist of unusual metal−sulfide-cluster frameworks.[1] Although the two active sites have been thought to play different roles in the enzymatic function of nitrogenase, their cluster cores show some intriguing structural similarities. One common feature is that a p-block atom connects two incomplete cubanes, each of which consists of four metal atoms and three sulfurs. The other common feature is hexa-coordination of the p-block atom encapsulated in a trigonal prismatic cage of six Fe atoms. The cluster core of FeMo-cofactor is formulated as $MoFe_7S_9X$ (X = C, N, or O), in which $[MoFe_3S_3]$ and $[Fe_4S_3]$ incomplete cubanes are linked by three S atoms and the hexa-coordinate X.[2] On the other hand, an S atom coordinates to six Fe atoms in the $[Fe_8S_7]$ core of P-cluster, and two $[Fe_3S_4]$ incomplete cubanes are bridged also by two cysteine S atoms. Although the structures of VFe-nitrogenase and Fe-nitrogenase are yet to be determined, close homology of their protein sequences to that of MoFe-nitrogenase indicates that the cofactors in VFe- and Fe-nitrogenases may be structurally analogous to the FeMo-cofactor.[3,4]

The unusual and intricate active-site structures of MoFe nitrogenase have been the long-standing synthetic targets for inorganic chemists.[5] A typical synthetic route to Fe/S and M/Fe/S (M = V, Mo) clusters of high nuclearity, which may mimic the cluster active sites of nitrogenases, is to aggregate preformed $[Fe_4S_4]$ and $[MFe_3S_4]$ cubane clusters by appropriate substitution and displacement reactions of terminal ligands. Using this approach, two independent research groups of D. Coucouvanis and R. H. Holm synthesized several intriguing double-cubane Fe/S and Mo/Fe/S clusters.[5a−d] We also reported the synthesis of a $[Mo_2Fe_2S_4]$ cubane cluster, $Cp^*_2Mo_2Fe_2S_4Cl_2$ ($Cp^* = \eta^5\text{-}C_5Me_5$), from the reaction between

(1) (a) Burgess, B. K.; Lowe, D. L. *Chem. Rev.* **1996**, *96*, 2983−3011. (b) Howard, J. B.; Rees, D. C. *Chem. Rev.* **1996**, *96*, 2965−2982. (c) Rees, D. C.; Howard, J. B. *Curr. Opin. Chem. Biol.* **2000**, *4*, 559−566.
(2) Einsle, O.; Tezcan, F. A.; Andrade, S. L. A.; Schmid, B.; Yoshida, M.; Howard, J. B.; Rees, D. C. *Science* **2002**, *297*, 1696−1700.
(3) (a) Bishop, P. E.; Premakumar, R. In *Biological Nitrogen Fixation;* Stacey, G., Burris, R. H., Evans, H. J., Eds.; Chapman & Hall: New York, 1992; pp 736−762. (b) Eady, R. R. *Chem. Rev.* **1996**, *96*, 3013−3030.
(4) (a) Chisnell, J. R.; Premakumaar, R.; Bishop, P. E. *J. Bacteriol.* **1988**, *170*, 27−33. (b) Kennedy, C.; Dean, D. *Mol. Gen. Genet.* **1992**, *231*, 494−498. (c) Schneider, K.; Gollan, U.; Dröttboom, M.; Selsemeier-Voigt, S.; Müller, A. *Eur. J. Biochem.* **1997**, *244*, 789−800. (d) Rüttimann-Johnson, C.; Rangaraj, P.; Shah, V. K.; Ludden, P. W. *J. Biol. Chem.* **2001**, *276*, 4522−4526. (e) Oda, Y.; Samanta, S. K.; Rey, F. E.; Wu, L.; Liu, X.; Yan, T.; Zhou, J.; Harwood, C. S. *J. Bacteriol.* **2005**, *187*, 7784−7794.
(5) Fe/S double-cubane clusters: (a) Challen, P. R.; Koo, S.-M.; Dunham, W. R.; Coucouvanis, D. *J. Am. Chem. Soc.* **1990**, *112*, 2455−2456. (b) Goh, C.; Segal, B. M.; Huang, J.; Long, J. R.; Holm, R. H. *J. Am. Chem. Soc.* **1996**, *118*, 11844−11853. Mo/Fe/S double-cubane clusters: (c) Demadis, K. D.; Campana, C. F.; Coucouvanis, D. *J. Am. Chem. Soc.* **1995**, *117*, 7832−7833. (d) Huang, J.; Mukerjee, S.; Segal, B. M.; Akashi, H.; Zhou, J.; Holm, R. H. *J. Am. Chem. Soc.* **1997**, *119*, 8662−8674. Mo/Fe/S clusters topologically analogous to P-cluster: (e) Zhang, Y.; Zuo, J.-L.; Zhou, H.-C.; Holm, R. H. *J. Am. Chem. Soc.* **2002**, *124*, 14292−14293. (f) Zhang, Y.; Holm, R. H. *J. Am. Chem. Soc.* **2003**, *125*, 3910−3920. (g) Zuo, J.-L.; Zhou, H.-C.; Holm. R. H. *Inorg. Chem.* **2003**, *42*, 4624−4631. (h) Zhang, Y.; Holm, R. H. *Inorg. Chem.* **2004**, *43*, 674−682.

$Cp^*Mo(S^tBu)_3$ and $FeCl_3$, and the subsequent aggregation into a cyclic tricubane cluster $[Cp^*_2Mo_2Fe_2S_4]_3(\mu\text{-}S_4)_3$ by treatment with Li_2S_2.[6]

On the other hand, skeletal rearrangement of fused double-cubane clusters $[MFe_3S_4]$ (M = Mo or V) was found to occur, generating a series of $[M_2Fe_6S_9]$ (M = Mo or V) clusters, the structures of which are topologically related to P-cluster.[5e−h] Recently, we succeeded in reproducing the $[Fe_8S_7]$ inorganic core structure of the reduced form of P-cluster by the synthesis of $[Fe_4S_3\{N(SiMe_3)_2\}(tmtu)_2]_2(\mu_6\text{-}S)\{\mu\text{-}N(SiMe_3)\}_2$ from a self-assembly reaction of $Fe\{N(SiMe_3)_2\}_2$,[7] tetramethylthiourea (*tmtu*), 2, 4, 6-triisopropylbenzenethiol, and elemental sulfur in toluene.[8] The P-cluster model, $[Fe_4S_3\{N(SiMe_3)_2\}(tmtu)_2]_2(\mu_6\text{-}S)\{\mu\text{-}N(SiMe_3)\}_2$, was found to decompose gradually into $[Fe_4S_4(SPh)_4]^{2-}$ in the presence of benzenethiol in acetonitrile, while the cluster complex is also labile under the presence of thiolate anions in polar solvents.

When the dithiol-promoted core extrusion method was applied to the MoFe-proteins of nitrogenases from *C. pasteurianum* and *A. vinelandii*, 90−103% of non-cofactor Fe content was extruded as $[Fe_4S_4(SR_F)_4]^{2-}$, after ligand exchange of the initial extrusion products with *p*-$CF_3C_6H_4SH$ (R_FSH), where the iron does not arise from the FeMo-co.[9] It was later suggested that, although P-clusters can be extruded once the protein is denatured, the P-clusters degrade into thermodynamically more stable cubane clusters in the extrusion process.[1b] On the other hand, ligand exchange reactions between $[Fe_4S_4(SPh)_4]^{2-}$ and $[Fe_4S_4Cl_4]^{2-}$ were reported to occur in DMF.[10] We speculate that the polar solvent causes a partial dissociation of thiolate, which in turn promotes the ligand exchange reaction, and that degradation of the P-cluster model might be initiated by a partial dissociation of thiolate in polar solvents. Thus, a key to the successful isolation of $[Fe_4S_3\{N(SiMe_3)_2\}(tmtu)_2]_2$ $(\mu_6\text{-}S)\{\mu\text{-}N(SiMe_3)\}_2$ would be the use of a nonpolar solvent in the reaction, toluene in our case. Another factor might be that the bulky thiolate ligand protects the metastable sulfide cluster from being attacked by nucleophiles, etc.

To expand the scope of cluster syntheses, we have been developing new methods to assemble Fe/S/thiolate and Fe/Mo/S/thiolate clusters of high nuclearity in nonpolar solvents. This paper describes isolation of a new class of $[Fe_8S_7]$ clusters, $[Fe_4S_3(SDmp)]_2(\mu\text{-}SDmp)_2(\mu\text{-}STip)(\mu_6\text{-}S)$ (**2**) (Tip = 2,4,6-^{i}Pr$_3$C$_6$H$_2$, Dmp = 2,6-(mesityl)$_2$C$_6$H$_3$), and $[Fe_4S_3(STip)]_2$-$(\mu\text{-}SDmp)_2\{\mu\text{-}N(SiMe_3)_2\}(\mu_6\text{-}S)$ (**3**), from the reaction of a preformed dinuclear iron(II) complex $[Fe(STip)(\mu\text{-}SDmp)]_2$ (**1**) with elemental sulfur, and from the one-pot reaction of $Fe\{N(SiMe_3)_2\}_2$, HSDmp, HSTip, and elemental sulfur. Having a hexacoordinate sulfur atom in the $[Fe_8S_7]$ core and three anionic ligands bridging Fe atoms of two incomplete $[Fe_4S_3]$ cubanes, the cluster structures of **2** and **3** are topologically analogous to FeMo-co and P-cluster, and they might also be relevant to the unknown FeFe-co structure of Fe-nitrogenase.

Scheme 1

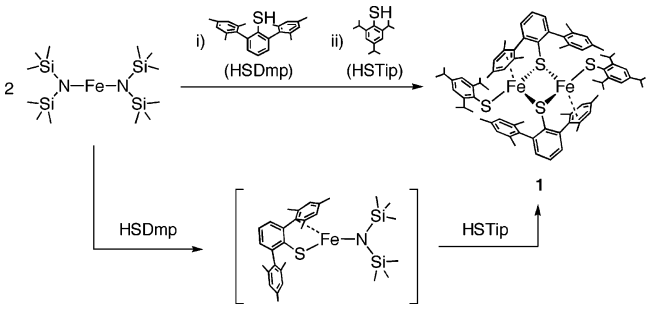

Results and Discussion

To construct unprecedented Fe/S/thiolate and Mo/Fe/S/thiolate clusters that mimic nitrogenase P-cluster and FeMo-cofactor, it is desirable to avoid formation of thermodynamically (or kinetically) stable cubane-type clusters. Among $[Fe_4S_4(SR)_4]^{n-}$ (n = 1−3) clusters, ubiquitous are dianionic $[Fe_4S_4(SR)_4]^{2-}$ forms with a formal $Fe(II)_2Fe(III)_2$ oxidation state, while $[Fe_4S_4(STip)_4]^-$ is a single example of an $Fe(II)Fe(III)_3$ cluster.[11] These anionic/dianionic clusters were generated from self-assembly reactions in polar solvents. On the other hand, neutral cubane clusters were synthesized in toluene, which include $[Fe_4S_4(CO)_{12}]$ $(Fe(II)_4)$,[12] $[Fe_4S_4\{N(SiMe_3)_2\}_4]$ $(Fe(III)_4)$,[13] and $[Fe_4S_4(STip)_2(tmtu)_2]$ $(Fe(II)_2Fe(III)_2)$.[14] The third cluster was isolated in >90% yield from (8:6:16:1) $Fe\{N(SiMe_3)\}_2$, tmtu, HSTip, and S_8, while the analogous reaction system with the molar ratio of (8:3:12:7/8) gave rise to an $[Fe_8S_7]$ cluster, $[Fe_4S_3$-$\{N(SiMe_3)_2\}(tmtu)_2]_2(\mu_6\text{-}S)\{\mu\text{-}N(SiMe_3)\}_2$ in 34% yield as crystals.[8] Here we set our prerequisites for the synthesis of metastable large clusters as (1) nonpolar solvent, (2) appropriate precursor with appropriate molar ratio, and (3) bulky thiolate ligand.

Synthesis and Structure of $[Fe(STip)(\mu\text{-}SDmp)]_2$ (1). Seeking for appropriate precursors for cluster synthesis, which are soluble in the nonpolar solvent, we have prepared a series of low-coordinate Fe(II) complexes of bulky thiolates from $Fe\{N(SiMe_3)_2\}_2$.[15] Here, the synthesis and structure of one such complex, $[Fe(STip)(\mu\text{-}SDmp)]_2$ (**1**), are described. Introduction of two different thiolates into one Fe(II) center was attained by the stepwise reaction of $Fe\{N(SiMe_3)_2\}_2$ with 1 equiv of HSDmp and 1 equiv of HSTip in toluene. In the first step of the reaction, the known thiolate/amide complex $Fe(SDmp)\{N(SiMe_3)_2\}$[16] was generated in situ, and the amide ligand reacted with HSTip to give **1** in 97% yield, as shown in Scheme 1. Obviously, it is important to react $Fe\{N(SiMe_3)_2\}_2$ first with bulkier thiol, for the high yield synthesis of **1**.

The X-ray crystallographic analysis revealed a dinuclear structure of **1**, as shown in Figure 1. Two SDmp ligands bridge two Fe(II) centers, and a crystallographic inversion center resides

(6) Kawaguchi, H.; Yamada, K.; Ohnishi, S.; Tatsumi, K. *J. Am. Chem. Soc.* **1997**, *119*, 10871−10872.
(7) Andersen, R. A.; Faegri, K., Jr.; Green, J. C.; Haaland, A.; Lappert, M. F.; Leung, W.-P.; Rypdal, K. *Inorg. Chem.* **1988**, *27*, 1782−1786.
(8) Ohki, Y.; Sunada, Y.; Honda, M.; Katada, M.; Tatsumi, K. *J. Am. Chem. Soc.* **2003**, *125*, 4052−4053.
(9) Kurts, D. M., Jr.; McMillan, R. S.; Burgess, B. K.; Mortenson, L. E.; Holm, R. H. *Proc. Natl. Acad. Sci. U.S.A.* **1979**, *76*, 4986−4989.
(10) Coucouvanis, D.; Kanatzidis, M.; Simhon, E.; Baenziger, N. C. *J. Am. Chem. Soc.* **1982**, *104*, 1874−1882.
(11) (a) O'Sullivan, T.; Millar, M. M. *J. Am. Chem. Soc.* **1985**, *107*, 4096−4097. (b) Papaefthymiou, V.; Millar, M. M.; Münck, E. *Inorg. Chem.* **1986**, *25*, 3010−3014.
(12) Nelson, L. L.; Lo, F. Y.-K.; Rae, A. D.; Dahl, L. F. *J. Organomet. Chem.* **1982**, *225*, 309−329.
(13) Ohki, Y.; Sunada, Y.; Tatsumi, K. *Chem. Lett.* **2005**, *34*, 172−173.
(14) Bicrbach, U.; Saak, W.; Haase, D.; Pohl, S. *Z. Naturforsch. B* **1991**, *46*, 1629−1634.
(15) Ohta, S.; Ohki, Y.; Ikagawa, Y.; Suizu, R.; Tatsumi, K. *J. Organomet. Chem.*, in press.
(16) (a) Ellison, J. J.; Rhulandt-Senge, K.; Power, P. P. *Angew. Chem., Int. Ed. Engl.* **1994**, *33*, 1178−1180. (b) Fe···C interaction in $Fe(SDmp)_2$ or $Fe(SDmp)\{N(SiMe_3)_2\}$ was indicated by Mössbauer spectrum: Evans, D. J.; Hughes, D. L.; Silver, J. *Inorg. Chem.* **1997**, *36*, 747−748.

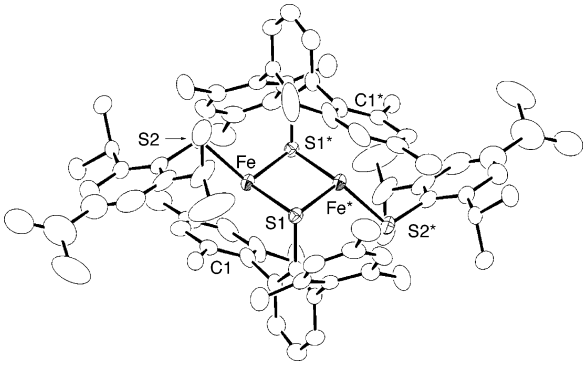

Figure 1. Molecular structure of $[(TipS)Fe(\mu\text{-}SDmp)]_2$ (**1**) with thermal ellipsoids at 50% probability level. Selected bond distances (Å) and angles (deg): Fe−Fe* = 3.0099(5), Fe−S1 = 2.3694(7), Fe−S2 = 2.2734(8), Fe−S1* = 2.3888(7), Fe−C1 = 2.532(2), Fe−S1−Fe* = 78.48(2), S1−Fe−S1* = 101.52, S1-Fe-S2 = 122.16(3), S1*−Fe−S2 = 111.92(2).

in the center of the Fe_2S_2 rhomboid. The Dmp substituents stands up and down from this Fe_2S_2 plane, with the S−C vectors being perpendicular to it. The Fe−Fe distance of 3.0099(5) Å is somewhat too long to invoke metal−metal interactions, although the Fe−S−Fe angle is acute. Two STip ligands each coordinates at an Fe atom from above or below the plane, completing a pyramidalized 3-coordinate geometry of Fe. One mesityl ring of each μ-SDmp orients in such a way that it caps Fe from the vacant site. Although the Fe−C distance of 2.532(3) Å is very long, coordinative unsaturation of the pyramidalized 3-coordinate Fe must be eased by noncovalent interactions with the mesityl ring. Such weak metal-to-carbon bonding is characteristic of bulky-arylthiolate complexes, e.g., $Fe(SDmp)\{N(SiMe_3)_2\}$ (Fe-*ipso*-C: 2.422−2.459 Å), $Fe(SDmp)_2$ (2.470(3), 2.535(3) Å), $Fe\{S\text{-}2,6\text{-}(2,4,6\text{-}^iPr_3C_6H_2)_2C_6H_3\}_2$ (2.427(1) Å), and Cp*Ru(SDmp) (Ru-*ipso*-C: 2.278(3) Å).[16−18]

Although divalent Fe bis-thiolate compounds tend to form oligomeric/polymeric structures $[Fe(\mu\text{-}SR)_2]_n$, the bulky thiolate substituents stabilize the dimeric structure of **1**, which in turn makes **1** highly soluble in nonpolar solvents. Complex **1** is air/moisture sensitive and it is also unstable in donor solvents, indicating coordinative unsaturation of **1**. Dark-red color of its toluene solution turns immediately dark brown when exposed to air, or even with adventitious contamination by air/moisture, while treatment of **1** in THF causes the color change from dark-red to yellow.

Synthesis of New $[Fe_8S_7]$ Clusters. Complex **1** was found to react with elemental sulfur in toluene to give a dark homogeneous solution. Removal of the solvent left a black oily material, and isolation of product(s) from it was a challenge. However, after seeking a suitable reaction condition and an appropriate solvent for recrystallization, we found that the reaction between **1** and $^1/_4$ equiv of S_8 in toluene for 4 days, followed by recrystallization from a 1:2 mixture of toluene and hexamethyldisiloxane (HMDSO), led to formation of black plates of $[Fe_4S_3(SDmp)]_2(\mu\text{-}SDmp)_2(\mu\text{-}STip)(\mu_6\text{-}S)$ (**2**) (Scheme 2). The new $[Fe_8S_7]$ cluster was isolated in 28% yield, and the molecular structure was determined by X-ray analysis. Prolonged reaction time appeared to be required to obtain **2** in moderate yield.

Scheme 2

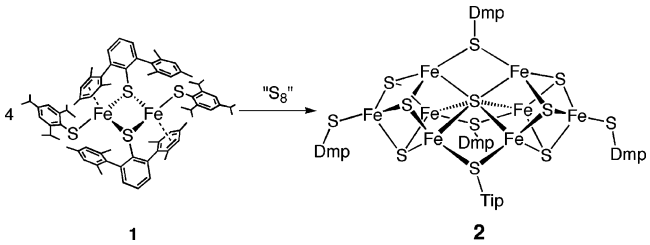

Scheme 3

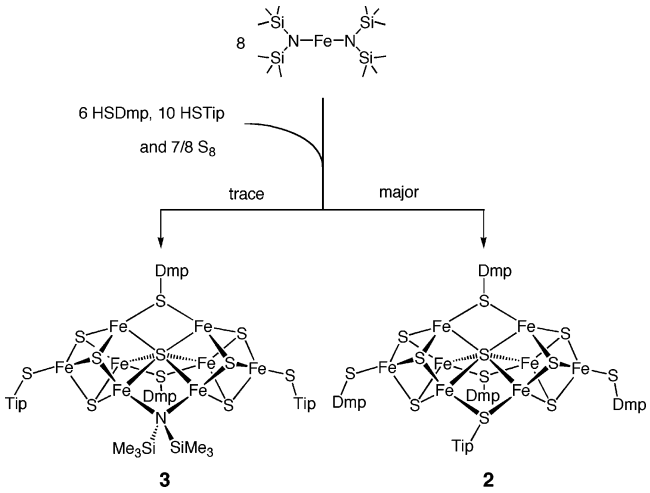

The neutral cluster **2** consists of eight Fe atoms with a formal oxidation state of $Fe(II)_5Fe(III)_3$. Thus, partial oxidation of Fe occurred in the reaction between **1** and S_8, and elemental sulfur must have served as an oxidant. On the other hand, a part of thiolates are to be eliminated presumably as disulfide, because the number of thiolates per Fe decreases from 2 to $^5/_8$ during the transformation of **1** into **2**. This elimination step causes reduction of Fe. The assembly of the $[Fe_8S_7]$ cluster core is thus achieved by the interplay between these oxidation and reduction processes. Whereas the reaction mechanism is not clear, the moderate yield of **2** indicates thermodynamic stability of the unprecedented cluster frame. It remains a possibility, however, that a multitude of neutral clusters other than **2** are formed in the reaction between **1** and S_8, and further attempts to isolate other products are in progress.

The successful isolation of **2** prompted us to examine a spontaneous cluster-assembly reaction of $Fe\{N(SiMe_3)_2\}_2$, HSDmp, HSTip, and S_8 in toluene (Scheme 3). A dark-brown solution of the (8:6:10:7/8) $Fe\{N(SiMe_3)_2\}_2$/HSDmp/HSTip/S_8 reaction mixture was stirred for 2 days, and the black residue obtained therefrom was subjected to crystallization. Crystallization from ether produced a small amount of black needles in addition to black plates of **2**. The X-ray crystallographic analysis of a black needle showed that the compound is another $[Fe_8S_7]$ cluster formulated as $[Fe_4S_3(STip)]_2(\mu\text{-}SDmp)_2\{\mu\text{-}N(SiMe_3)_2\}(\mu_6\text{-}S)$ (**3**). Although the majority of crystals obtained from ether are those of complex **2**, black needles of **3** were found to be predominat when crystallized from a concentrated toluene solution. The reaction of preformed $Fe_3\{N(SiMe_3)_2\}_2(\mu\text{-}STip)_4$[19] with HSDmp and S_8 for 2 days,

(17) Nguyen, T.; Panda, A.; Olmstead, M. M.; Richards, A. F.; Stender, M.; Brynda, M.; Power, P. P. *J. Am. Chem. Soc.* **2005**, *127*, 8545−8552.
(18) Ohki, Y.; Sadohara, H.; Takikawa, Y.; Tatsumi, K. *Angew. Chem., Int. Ed.* **2004**, *43*, 2290−2293.
(19) MacDonnell, F. M.; Ruhlandt-Senge, K.; Ellison, J. J.; Holm, R. H.; Power, P. P. *Inorg. Chem.* **1995**, *34*, 1815−1822.

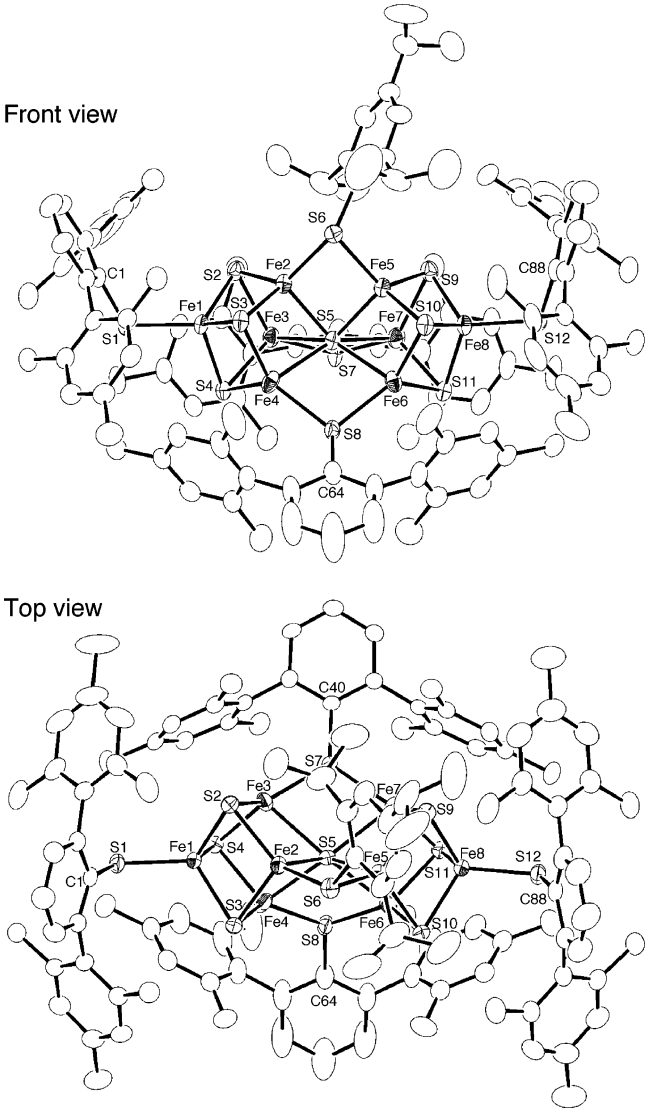

Figure 2. Two molecular views of $[(DmpS)Fe_4S_3]_2(\mu\text{-SDmp})_2(\mu\text{-STip})(\mu_6\text{-S})$ (**2**) with thermal ellipsoids at 50% probability level.

followed by a workup and crystallization similar to those described above, also generated **2** along with a small amount of **3**.

As will be discussed later in this paper, compounds **2** and **3** have very similar $[Fe_8S_7]$ core geometries with a common $Fe(II)_5Fe(III)_3$ oxidation state. Both **2** and **3** were generated from the two independent self-assembly reactions, and the reaction of **1** and S_8 also yielded **2**. These experiments suggest that the unusual $[Fe_8S_7]$ cluster structure may be a thermodynamically stable form led by a multitude of transformations occurring in the self-assembly reactions. Use of a nonpolar solvent in these reactions appears to be important for the construction of the $[Fe_8S_7]$ clusters.

Molecular Structures of 2 and 3. The X-ray derived molecular structure of **2** is shown in Figure 2, and the selected geometric parameters except for the interatomic distances in the $[Fe_8(\mu\text{-S})]$ skeletons are listed in Table 1. The molecule consists of two Fe_4S_3 incomplete cubane units, which are connected by one μ_6-S and three thiolate S atoms. Of the three thiolate bridges, two are SDmp and one is STip. In addition, two SDmp ligands coordinate at the two outer Fe atoms of the cluster core, and all Fe atoms in the cluster assume distorted tetrahedral coordination geometries. The bulky μ-SDmp groups sandwich the $[Fe_8S_7]$ cluster from the bottom, and the Dmp groups of the terminal thiolates are both sticking upward to avoid steric congestion of the μ-SDmp. Although the Fe−S distances associated with the μ-STip and μ-SDmp bridges are in a narrow range of 2.3015(10) to ~2.3299(14) Å, the Fe−S(μ-STip)−Fe angle (77.87(3)°) is markedly smaller than the Fe−S(μ-SDmp)−Fe angles (102.10(4)° and 105.73(4)°). Another interesting geometrical feature is the Tip group of μ-STip, which tilts substantially from a symmetric orientation. The cause of the tilting is not clear, whether it is due to the electronic property characteristic of the $[Fe_8S_7]$ core or due to a packing effect. However, we point out here that one hexamethyldisiloxane (HMDSO) molecule sits in the void created by the tilt of Tip as a crystal solvent. Yet another intriguing feature to be mentioned is the planar geometry of the μ-SDmp sulfurs, which would enhance the p_π-donor ability of the thiolate ligand.

In cluster **3**, an amide nitrogen and two SDmp sulfurs bridge Fe atoms of the two incomplete Fe_4S_3 cores, and terminal thiolate ligands are now STip (Figure 3). Except for the different ligand arrangement, the overall cluster structure of **3** is very similar to that of **2**. Among the three bridging ligands, the Fe−N(μ-amide)−Fe angle is acute (86.7(4)°) and the Fe−S(μ-SDmp)−Fe angle is large (104.92(14)°), as was the case for μ-STip and μ-SDmp of **2**, respectively. This geometrical feature is discussed later in this section. Note that a crystallographic C_2 axis runs through N, μ_6-S, and the midpoint between two μ-S atoms in the structure of **3**, which was crystallized with *C*2/*c* space group. The selected bond distances and angles are given in Table 2, except for Fe−Fe and Fe-(μ_6-S) distances shown in Figure 4.

Figure 4 compares the cluster cores of **2** and **3**, where the interatomic distances in their $[Fe_8(\mu\text{-S})]$ skeletons are given. The $[MoFe_7S_9X]$ core geometry of FeMo-co[2] is also shown in the figure for comparison. For either **2** or **3**, the $[Fe_8(\mu\text{-S})]$ skeleton may be viewed as a bicapped trigonal prism, and one S atom is encapsulated in the distorted trigonal prismatic array of six Fe atoms. Of the three Fe−Fe edges, which connect two trigonal faces within the distorted trigonal prism, two are very long (3.6196(10)−3.7050(10) Å). The long edges are where SDmp ligands bridge, while the short Fe−Fe edge is bridged by either STip (2.9103(10) Å) or $N(SiMe_3)_2$ (2.804(2) Å). The long Fe−Fe distances result in elongation of the Fe−μ_6-S bond distances. The distortion might be ascribed to the steric bulk of Dmp, or μ_6-S might be too large to hold six Fe atoms tightly all together, while there is also a possibility that electronic property of the cluster core induces such distortion.

The clusters **2** and **3** have intriguing structural relevance to the nitrogenase FeMo-co, in that two $[M_4S_3]$ incomplete cubanes are connected by a μ_6-X atom and three bridging ligands. For FeMo-co, X is a light element atom postulated as C, N, or O instead of S,[2,20] and bridging ligands are sulfides (S^{2-}) instead of thiolate sulfurs, and one incomplete cubane is $[MoFe_3S_3]$ instead of $[Fe_4S_3]$. Despite these obvious differences, the cluster structures of **2** and **3** are topologically analogous to that of FeMo-co, and the two structures are compared in more detail.

(20) (a) Lee, H.-L.; Benton, P. M. C.; Laryukhin, M.; Igarashi, R. Y.; Dean, D. R.; Seefeldt, L. C.; Hoffman, B. M. *J. Am. Chem. Soc.* **2003**, *125*, 5604−5605. (b) Yang, T.-C.; Maeser, N. K.; Laryukhin, M.; Lee, H.-I.; Dean, D. R.; Seefeldt, L. C.; Hoffman, B. M. *J. Am. Chem. Soc.* **2005**, *127*, 12804−12805.

Table 1. Selected Bond Distances (Å) and Angles (deg) for **2**[a]

Fe(1)−S(1)	2.2336(13)	S(1)−Fe(1)−S(2)	118.94(5)	S(5)−Fe(6)−S(7)	75.64(4)	Fe(2)−S(5)−Fe(6)	129.95(5)
Fe(1)−S(2)	2.2795(12)	S(1)−Fe(1)−S(3)	117.64(4)	S(5)−Fe(6)−S(9)	100.22(4)	Fe(2)−S(5)−Fe(7)	133.90(4)
Fe(1)−S(3)	2.2876(12)	S(1)−Fe(1)−S(4)	107.37(4)	S(5)−Fe(6)−S(11)	101.64(4)	Fe(3)−S(5)−Fe(4)	75.58(3)
Fe(1)−S(4)	2.2628(11)	S(2)−Fe(1)−S(3)	103.33(4)	S(7)−Fe(6)−S(9)	131.90(5)	Fe(3)−S(5)−Fe(5)	133.82(5)
Fe(2)−S(2)	2.2576(13)	S(2)−Fe(1)−S(4)	103.37(4)	S(7)−Fe(6)−S(11)	125.17(4)	Fe(3)−S(5)−Fe(6)	99.58(4)
Fe(2)−S(3)	2.2802(12)	S(3)−Fe(1)−S(4)	104.45(4)	S(9)−Fe(6)−S(11)	102.78(4)	Fe(3)−S(5)−Fe(7)	150.95(4)
Fe(2)−S(6)	2.3296(11)	S(2)−Fe(2)−S(3)	104.27(4)	S(5)−Fe(7)−S(8)	77.60(4)	Fe(4)−S(5)−Fe(5)	131.08(4)
Fe(3)−S(2)	2.2903(12)	S(2)−Fe(2)−S(5)	107.68(4)	S(5)−Fe(7)−S(10)	100.79(4)	Fe(4)−S(5)−Fe(6)	150.59(4)
Fe(3)−S(4)	2.2912(12)	S(2)−Fe(2)−S(6)	129.07(4)	S(5)−Fe(7)−S(11)	101.84(4)	Fe(4)−S(5)−Fe(7)	96.04(4)
Fe(3)−S(7)	2.3235(12)	S(3)−Fe(2)−S(5)	100.49(4)	S(8)−Fe(7)−S(10)	135.36(4)	Fe(5)−S(5)−Fe(6)	73.13(3)
Fe(4)−S(3)	2.2867(11)	S(3)−Fe(2)−S(6)	110.78(4)	S(8)−Fe(7)−S(11)	120.51(4)	Fe(5)−S(5)−Fe(7)	72.42(3)
Fe(4)−S(4)	2.2750(12)	S(5)−Fe(2)−S(6)	101.03(4)	S(10)−Fe(7)−S(11)	103.64(4)	Fe(6)−S(5)−Fe(7)	73.96(4)
Fe(4)−S(8)	2.3299(14)	S(2)−Fe(3)−S(4)	102.13(4)	S(9)−Fe(8)−S(10)	103.86(4)	Fe(2)−S(6)−Fe(5)	77.87(3)
Fe(5)−S(6)	2.3015(12)	S(2)−Fe(3)−S(5)	102.34(4)	S(9)−Fe(8)−(11)	103.57(4)	Fe(2)−S(6)−C(25)	131.52(16)
Fe(5)−S(9)	2.2479(13)	S(2)−Fe(3)−S(7)	133.22(4)	S(9)−Fe(8)−S(12)	117.39(4)	Fe(5)−S(6)−C(25)	103.69(14)
Fe(5)−S(10)	2.2512(13)	S(4)−Fe(3)−S(5)	99.76(4)	S(10)−Fe(8)−S(11)	104.24(4)	Fe(3)−S(7)−Fe(6)	105.73(4)
Fe(6)−S(7)	2.3241(12)	S(4)−Fe(3)−S(7)	124.50(4)	S(10)−Fe(8)−S(12)	115.13(4)	Fe(3)−S(7)−C(40)	122.77(16)
Fe(6)−S(9)	2.2813(11)	S(5)−Fe(3)−S(7)	75.39(4)	S(11)−Fe(8)−S(12)	111.22(4)	Fe(6)−S(7)−C(40)	122.92(14)
Fe(6)−S(11)	2.2863(14)	S(3)−Fe(4)−S(4)	104.09(5)	Fe(1)−S(1)−C(1)	116.06(13)	Fe(4)−S(8)−Fe(7)	102.10(4)
Fe(7)−S(8)	2.3237(12)	S(3)−Fe(4)−S(5)	96.18(4)	Fe(1)−S(2)−Fe(2)	74.48(4)	Fe(4)−S(8)−C(64)	121.15(17)
Fe(7)−S(10)	2.2859(10)	S(3)−Fe(4)−S(8)	135.47(4)	Fe(1)−S(2)−Fe(3)	75.31(4)	Fe(7)−S(8)−C(64)	121.27(16)
Fe(7)−S(11)	2.2730(12)	S(4)−Fe(4)−S(5)	99.90(4)	Fe(2)−S(2)−Fe(3)	75.58(4)	Fe(5)−S(9)−Fe(6)	76.70(4)
Fe(8)−S(9)	2.2828(14)	S(4)−Fe(4)−S(8)	120.44(4)	Fe(1)−S(3)−Fe(2)	73.89(4)	Fe(5)−S(9)−Fe(8)	72.99(4)
Fe(8)−S(10)	2.2803(12)	S(5)−Fe(4)−S(8)	77.14(4)	Fe(1)−S(3)−Fe(4)	74.80(3)	Fe(6)−S(9)−Fe(8)	75.27(4)
Fe(8)−S(11)	2.2599(10)	S(5)−Fe(5)−S(6)	102.03(4)	Fe(2)−S(3)−Fe(4)	80.54(4)	Fe(5)−S(10)−Fe(7)	75.91(3)
Fe(8)−S(12)	2.2272(13)	S(5)−Fe(5)−S(9)	105.13(4)	Fe(1)−S(4)−Fe(3)	75.62(3)	Fe(5)−S(10)−Fe(8)	72.97(4)
		S(5)−Fe(5)−S(10)	105.99(4)	Fe(1)−S(4)−Fe(4)	75.50(3)	Fe(7)−S(10)−Fe(8)	74.33(3)
		S(6)−Fe(5)−S(9)	120.70(4)	Fe(3)−S(4)−Fe(4)	81.72(4)	Fe(6)−S(11)−Fe(7)	79.46(4)
		S(6)−Fe(5)−S(10)	115.53(4)	Fe(2)−S(5)−Fe(3)	72.10(4)	Fe(6)−S(11)−Fe(8)	75.62(4)
		S(9)−Fe(5)−S(10)	105.96(5)	Fe(2)−S(5)−Fe(4)	76.92(4)	Fe(7)−S(11)−Fe(8)	74.97(3)
				Fe(2)−S(5)−Fe(5)	78.59(3)	Fe(8)−S(12)−C(88)	110.97(15)

[a] Fe−Fe and Fe−(μ_6-S) distances given in Figure 4 are omitted in this table.

In the case of FeMo-co, the trigonal prism made of six inner Fe atoms is not distorted, and Fe−Fe distances are all rather short. The size of the prismatic cage is ideally situated so as to accommodate one light element X. A large sulfur atom cannot be encapsulated in this cage, and the consequence is the distortion/expansion of the Fe_6 prismatic cage, as can be seen in the structures of **2** and **3**, that is, elongation of two Fe−Fe distances. Coping with the long Fe−Fe distances, the Fe−S(μ-SDmp)−Fe angles of **2** and **3** (102.10(4)°−105.73(4)°) are substantially larger than the Fe−(μ-S)-Fe angles of FeMo-co (71.0−71.8°). In other words, two incomplete cubane cores of **2** and **3** bend away from each other with one short intercubane Fe−Fe bond being as a pivotal axis. The Fe−S(μ-STip)−Fe and Fe−N(μ-amide)−Fe angles (77.87(3)° and 86.7(4)°) are also larger than the Fe-(μ-S)−Fe angles of FeMo-co. The Fe−Fe bond distances within the incomplete cubanes (**2**, av 2.816 Å; **3**, av 2.831 Å) are also somewhat longer compared with the corresponding Fe(Mo)−Fe distances (av 2.69 Å) of FeMo-co. To visualize these structural similarity/difference between **2**, **3**, and FeMo-co, their wireframe views are superimposed in Figure 5. The entire cluster cores of **2** and **3** are evidently larger than that of FeMo-co. The separation between the outer Fe atoms are 7.7542(8) (**2**) and 7.729(2) Å (**3**), while the corresponding Mo−Fe separation of FeMo-co is 7.01 Å.

Electronic Properties of 2 and 3. According to the polyhedral skeletal electron pair theory (PSEP theory),[21] octanuclear clusters with 114 electrons are electron precise for the bicapped-trigonal-prism (btp) structure, while 118 electrons are needed for a btp structure with two long metal−metal distances as in the case of the structure of **2**. Cluster **2** (and **3** as well**)** has 105 valence electrons within its cluster framework, that is, 45($Fe(II)_5Fe(II)_3$) + 36 (6 × μ_3-S) + 8(μ_6-S) + 12(3 × μ-SAr) + 4(2 × SAr), which is obviously electron deficient. Iron sulfur clusters, that exhibit functions of electron-transfer processes in metalloenzymes, are always electron deficient, which account for the unique function of the iron-sulfur clusters in the electron-transfer processes. For example, ubiquitous cubane clusters, $[Fe_4S_4(SR)_4]^{2-}$, carry 54 electrons, while 60 electrons are needed for tetranuclear clusters to be electron precise by the PSEP theory. The cluster structure of **2** and **3** may be viewed as a fused form of two $[Fe_4S_4(SR)_4]^{2-}$ units, and in the transformation from two cubanes to the $[Fe_8S_7]$ cluster of **2**, one μ_3-S (6-electron donor) becomes μ_6-S (8-electron donor) and three terminal thiolates (2-electron donor each) become μ-thiolates (4-electron donor each), while one μ_3-S and three thiolates are removed. Therefore, if the electron count of the cluster **2** is to be analogous to that of $[Fe_4S_4(SR)_4]^{2-}$, the number of cluster electrons for **2** is to be 104 = (2 × 54) + (8 − 6) + 3 × (4 − 2) − 6 − 3 × 2. The actual number of cluster electrons for **2** (105) is very close to it, suggesting that cluster **2** is electrochemically active, or at least as active as $[Fe_4S_4(SR)_4]^{2-}$. In fact, the cyclic voltammogram of **2**, measured in THF on a glassy carbon electrode with $(Bu_4N)(PF_6)$ as supporting electrolyte, shows well-separated three quasireversible reduction processes at $E_{1/2}$ = −0.74, −1.15, and −2.00 V (vs Cp_2Fe/Cp_2Fe^+).

An interesting aspect of the electronic structures of **2** and **3** is that they have an odd number of d-electrons with the common oxidation state of $Fe(II)_5Fe(III)_3$. The EPR spectrum of **2** at 10 K in frozen toluene exhibited a rhombic resonance at g = 2.19,

(21) (a) Wade, K. In *Transition Metal Clusters;* Johnson, F. B. G., Ed.; Wiley: New York, 1980; p 193. (b) For, a general discussion on the isolobal analogy: Hoffmann, R. *Angew. Chem., Int. Ed. Engl.* **1982**, *21*, 711−724. (c) Mingos, D. M. P.; Wales, D. J. In *Introduction to Cluster Chemistry;* Prentice Hall: Englewood Cliffs, NJ, 1990.

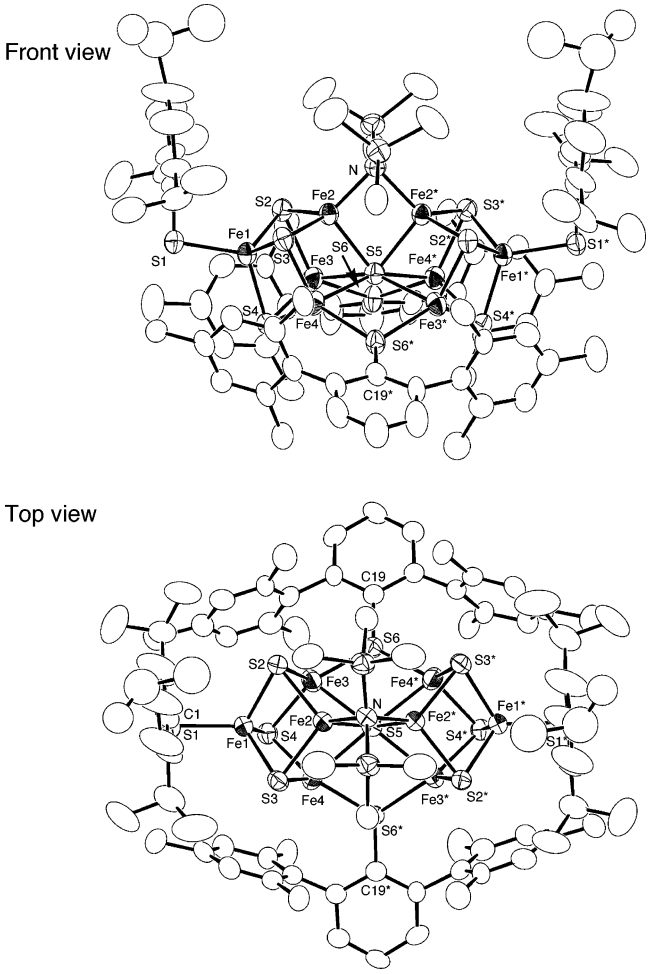

Figure 3. Two molecular views of $[(TipS)Fe_4S_3]_2(\mu\text{-}SDmp)_2\{\mu\text{-}N(SiMe_3)_2\}(\mu_6\text{-}S)$ (**3**) with thermal ellipsoids at 50% probability level.

2.07, 1.96, as shown in Figure 6. The EPR signal of **3** was also observed to be rhombic with $g = 2.13, 2.06, 1.93$, to which a set of weak signals associated with **2** mixed in, indicating that the sample of **3** used for the EPR measurement was slightly contaminated by **2**. The EPR spectra of **2** and **3** are compared with those of $[Fe_4S_4]^{n+}$ ($n = 1, 3$) clusters, P-cluster of MoFe nitrogenase, and FeFe-co of Fe-only nitrogenase, in $S = {}^1/_2$ states.

For naturally occurring iron−sulfur cubane clusters, the $[Fe_4S_4]^{3+}$ centers of HiPIP have been reported to exhibit axial EPR spectra, the *g*-values of which vary little from one protein to another with $g_{||} = 2.11-2.14$ and $g_{\perp} = 2.03-2.04$,[23] whereas the reduced forms of ferredoxins, $[Fe_4S_4]^{+}$, show rhombic or axial EPR signals with g_{av} values being in the region of 1.96−1.98.[24] It appears that the iron−sulfur clusters with higher oxidation states of Fe tend to give higher g_{av} values. This is also the case for synthetic $[Fe_4S_4]^{n+}$ ($n = 1, 3$) or $[Fe_4S_4(SR)_4]^{m-}$ ($m = 3, 1$) clusters. The oxidized iron−sulfur clusters, namely $[Fe_4S_4(SR)_4]^{-}$, have been reported to show rhombic EPR signals with $g_{av} = 2.00-2.06$.[11,25] On the other hand, the EPR signals of the reduced clusters $[Fe_4S_4(SR)_4]^{3-}$ are either rhombic (for R = H) or axial (majority), or isotropic, where the g_{av} values are in 1.92−1.98 region, while there is some complication in their EPR spectra because of the admixture of $S = {}^1/_2$ and $S = {}^3/_2$ spin states.[22,26]

While the reduced form of P-cluster (P^N) is EPR silent, the transient $S = {}^1/_2$ signals (rhombic, $g_{av} = 1.94$) for the partially oxidized MoFe proteins from *Klebsiella pneumoniae* (Kp1) and *A. vinelandii* ($Av1^{Mo}$) have been assigned to arise from the one-electron oxidized P-cluster (P^{1+}). Because eight iron atoms of P^N are thought to be all ferrous based on the Mössbauer study, one-electron oxidized form of P-cluster would consist of 7Fe(II) + Fe(III). The relatively high g_{av} values of rhombic EPR signals for **2** ($g_{av} = 2.07$) and **3** ($g_{av} = 2.04$) are not inconsistent with the $Fe(II)_5Fe(III)_3$ oxidation state of these clusters.

The Fe-only nitrogenase (FeFe protein) was isolated from *Rhodobacter capsulatus* and the detailed EPR study was reported.[27] For the various forms of Fe-only nitrogenase generated by oxidation/reduction of the protein, there appeared three significant $S = {}^1/_2$ bands upon oxidation. One such EPR band is a rhombic resonance at $g = 2.22, 2.05$, and 1.86 detected under a weakly acidic condition (pH 6.4), which happens to be close to the EPR signals of **2** and **3**. Another $S = {}^1/_2$ band was observed at $g = 1.96, 1.92$, and 1.77 for the dithionite-reduced state in "turnover" conditions. These $S = {}^1/_2$ EPR signals are unique to the FeFe protein, because the related MoFe protein under analogous conditions did not show these signals, and they might be originated from FeFe-cofactor. In this regard, similarity of the EPR signals of **2** and **3** to those of FeFe protein is intriguing, as FeFe-cofactor is suggested to be structurally similar to the FeMo-cofactor.[4,28]

Implication in the Core Structures of P-Cluster, FeMo-co, and FeFe-co. The topological analogy between the cluster structures of **2** (and **3**) and the nitrogenase FeMo-co has been emphasized early in this paper. One may also recognize that cluster **2** has structural relevance to P-cluster, with slight differences in their [8Fe-7S] core geometries and in the ligand arrangements. Cluster **2** carries five thiolate ligands, while the inorganic P-cluster core is bound to six cysteine sulfurs.[29] Thus, addition of a thiolate ligand to one of the inner iron atoms of **2** would lead to the P-cluster core structure. The array of inner six irons of **2** is distorted from the ideal trigonal prism, owing to encapsulation of a large μ_6-S atom, so that one of the Fe−S(μ-thiolate) bonds may be easily cleaved by an incoming thiolate. One obvious point at issue of this argument is that the electron count of the cluster obtained therefrom differs from that of P-cluster either in its reduced form (P^N) or a doubly

(22) Lakowski, E. J.; Frankel, R. B.; Gillum, W. O.; Papaefthymiou, G. C.; Renaud, J.; Ibers, J. A.; Holm, R. H. *J. Am. Chem. Soc.* **1978**, *100*, 5322−5337.
(23) (a) Dunham, W. R.; Hagen, W. R.; Fee, J. A.; Sands, R. H.; Dunbar, J. B.; Humblet, C. *Biochim. Biophys. Acta* **1991**, *1079*, 253−262. (b) Schoepp, B.; Parot, P.; Menin, L.; Gaillard, J.; Richaud, P.; Vermeglio, A. *Biochemistry* **1995**, *34*, 11736−11742. (c) Cavazza, C.; Guigliarelli, B.; Bertrand, P.; Bruschi, M. *FEMS Microbiol. Lett.* **1995**, *130*, 193−200.
(24) Guigliarelli, B.; Bertrand, P. *Adv. Inorg. Chem.* **1999**, *47*, 421−497.
(25) Pape, L. L.; Lamotte, B.; Mouesca, J.-M.; Rius, G. *J. Am. Chem. Soc.* **1997**, *119*, 9757−9770.
(26) (a) Laskowski, E. J.; Reynolds, J. G.; Frankel, R. B.; Foner, S.; Papaefthymiou, G. C.; Holm, R. H. *J. Am. Chem. Soc.* **1979**, *101*, 6562−6570. (b) Segal, B. M.; Hoveyda, H. R.; Holm, R. H. *Inorg. Chem.* **1998**, *37*, 3440−3443.
(27) Siemann, S.; Schneider, K.; Dröttboom, M.; Müller, A. *Eur. J. Biochem.* **2002**, *269*, 1650−1661.
(28) (a) Schüdderkopf, K.; Hennecke, S.; Liese, U.; Kutsch, M.; Klipp, W. *Mol. Microbiol.* **1993**, *8*, 673−684. (b) Krahn, E.; Weiss, B. J. R.; Kröckel, M.; Groppe, J.; Henkel, G.; Cramer, S. P.; Trautwein, A. X.; Schneider, K.; Müller, A. *J. Biol. Inorg. Chem.* **2002**, *7*, 37−45.
(29) The oxidized form of P-cluster (P^{OX}) is claimed to contain a coordinated carboxiamido-nitrogen from the peptide backbone. (a) Peters, J. W.; Stowell, M. H. B.; Soltis, S. M.; Finnegan, M. G.; Johnson, M. K.; Rees, D. C. *Biochemistry* **1997**, *36*, 1181−1187. (b) Mayer, S. M.; Lawson, D. M.; Gormal, C. A.; Roe, S. M.; Smith, B. E. *J. Mol. Biol.* **1999**, *292*, 871−891.

Table 2. Selected Bond Distances (Å) and Angles (deg) for **3**[a]

Fe(1)−S(1)	2.232(2)	S(1)−Fe(1)−S(2)	113.83(14)	S(4)−Fe(3)−S(5)	99.54(12)	Fe(2)−S(3)−Fe(4)	77.71(9)
Fe(1)−S(2)	2.269(3)	S(1)−Fe(1)−S(3)	113.89(12)	S(4)−Fe(3)−S(6)	128.06(11)	Fe(1)−S(4)−Fe(3)	74.46(9)
Fe(1)−S(3)	2.266(4)	S(1)−Fe(1)−S(4)	115.28(10)	S(5)−Fe(3)−S(6)	76.90(10)	Fe(1)−S(4)−Fe(4)	74.82(10)
Fe(1)−S(4)	2.265(2)	S(2)−Fe(1)−S(3)	102.87(11)	S(3)−Fe(4)−S(4)	103.14(13)	Fe(3)−S(4)−Fe(4)	81.11(10)
Fe(2)−S(2)	2.282(4)	S(2)−Fe(1)−S(4)	105.04(10)	S(3)−Fe(4)−S(5)	100.82(11)	Fe(2)−S(5)−Fe(2)*	74.20(11)
Fe(2)−S(3)	2.267(2)	S(3)−Fe(1)−S(4)	104.66(14)	S(3)−Fe(4)−S(6)*	130.02(15)	Fe(2)−S(5)−Fe(3)	73.97(6)
Fe(2)-N	2.042(8)	S(2)−Fe(2)−S(3)	102.44(12)	S(4)−Fe(4)−S(5)	99.42(10)	Fe(2)−S(5)−Fe(3)*	129.99(11)
Fe(3)−S(2)	2.283(3)	S(2)−Fe(2)−S(5)	104.08(9)	S(4)−Fe(4)−S(6)*	126.69(11)	Fe(2)−S(5)−Fe(4)	73.76(5)
Fe(3)−S(4)	2.292(2)	S(2)−Fe(2)−N	122.06(13)	S(5)−Fe(4)−S(6)*	76.81(8)	Fe(2)−S(5)−Fe(4)*	128.88(11)
Fe(3)−S(6)	2.317(2)	S(3)−Fe(2)−S(5)	104.61(9)	Fe(2)-N−Fe(2)*	86.7(4)	Fe(3)−S(5)−Fe(3)*	153.43(16)
Fe(4)−S(3)	2.283(2)	S(3)−Fe(2)−N	121.43(14)	Fe(1)−S(1)−C(1)	100.2(3)	Fe(3)−S(5)−Fe(4)	75.76(7)
Fe(4)−S(4)	2.296(4)	S(5)−Fe(2)−N	99.6(2)	Fe(1)−S(2)−Fe(2)	74.75(12)	Fe(3)−S(5)−Fe(4)*	98.38(7)
Fe(4)−S(6)*	2.320(3)	S(2)−Fe(3)−S(4)	103.74(9)	Fe(1)−S(2)−Fe(3)	74.57(10)	Fe(4)−S(5)−Fe(4)*	154.80(16)
		S(2)−Fe(3)−S(5)	100.82(13)	Fe(2)−S(2)−Fe(3)	77.61(12)	Fe(3)−S(6)−Fe(4)*	104.92(14)
		S(2)−Fe(3)−S(6)	128.03(11)	Fe(1)−S(3)−Fe(2)	75.12(12)	Fe(3)−S(6)−C(19)	124.4(3)
				Fe(1)−S(3)−Fe(4)	75.07(11)	Fe(4)−S(6)−C(19)	124.3(3)

[a] Fe−Fe and Fe-(μ_6-S) distances given in Figure 4 are omitted in this table.

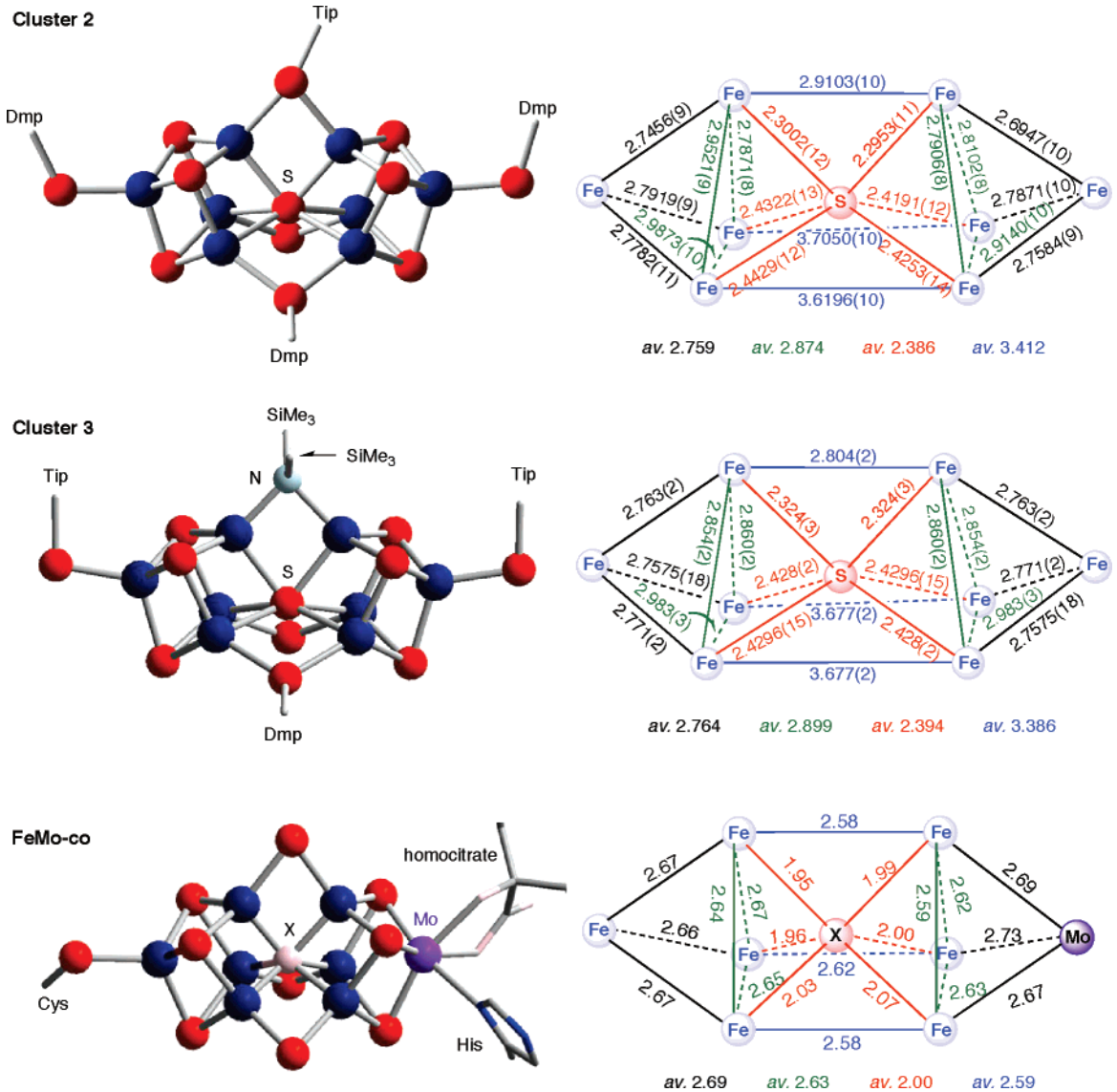

Figure 4. Comparison of the $[Fe_8S_7(\mu\text{-SAr})_3]$, $[Fe_8S_7(\mu\text{-SAr})_2\{\mu\text{-N(SiMe}_3)_2\}]$, and $[MoFe_7S_9]$ core geometries of **2**, **3**, and FeMo-co,[2] respectively.

oxidized form (P^{ox}). The formal oxidation state of irons in **2**(*SR*)-(−) would be $Fe(II)_5Fe(III)_3$, while P^N and P^{ox} consist of $Fe(II)_8$ and $Fe(II)_6Fe(III)_2$, respectively. Therefore, when cluster **2** is to be converted into P-cluster, one or three electron(s) should be provided. Nonetheless, **2** may be regarded as a key cluster linking conceptually FeMo-co and P-cluster, and Chart 1 summarizes their structural relationship.

Although the chemical formula and structure of FeFe-cofactor are yet unknown, cluster **2** may not be very far from the inorganic core frame of FeFe-cofactor. In order to gain further

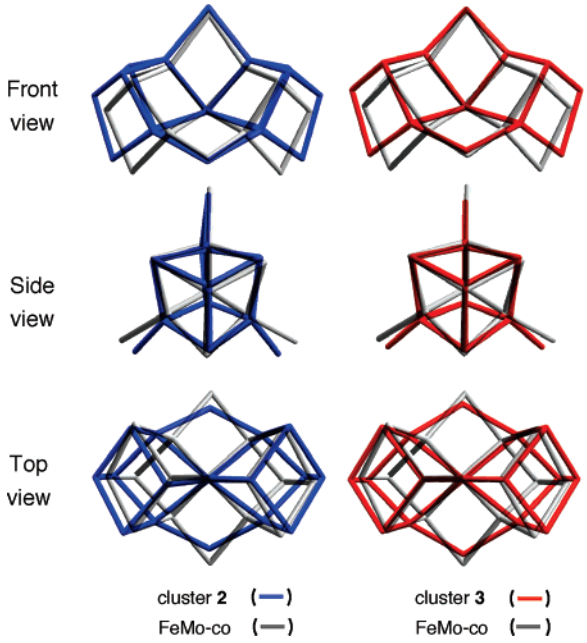

Figure 5. Superposition of the wire-frame core structures of **2** (blue), **3** (red), and FeMo-co (gray).

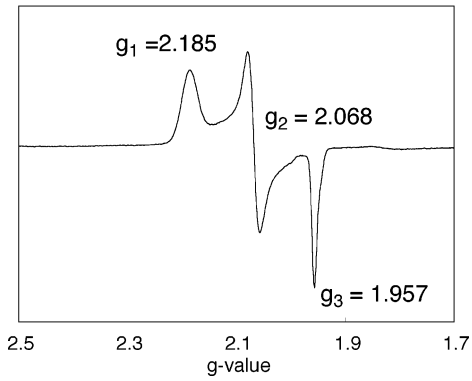

Figure 6. EPR spectrum of **2** (X-band, microwave 1.0 mW) in frozen toluene at 10 K.

insights into the fascinating structures and function of nitrogenases, it is desirable to develop new synthetic methods generating the complicated cluster structures of their active sites. In this regard, construction of transition metal sulfide clusters in a nonpolar solvent appears to be promising. In this study, a preformed coordinatively unsaturated iron-thiolate complex was found to react readily with elemental sulfur, giving rise to the unusual cluster forms in a self-assembly manner. Important facets of this synthetic strategy are that the reactions are rather straightforward and that the reaction conditions and iron-thiolate precursors can be modified from which a variety of unprecedented cluster structures could be produced.

Experimental Section

General Procedures. All reactions and manipulations were performed under nitrogen using glove boxes and standard Schlenk techniques. Hexane, toluene, and Et_2O were purified by the method of Grubbs, where the solvents were passed over columns of activated alumina and supported copper catalyst supplied by Hansen & Co. Ltd. Degassed and distilled solvents from sodium benzophenone ketyl (hexamethyldisiloxane, hexane, and toluene) were also used. UV−vis spectra were measured on a JASCO V560 spectrometer. Elemental analyses were performed on a LECO CHNS-932 microanalyzer where

Chart 1

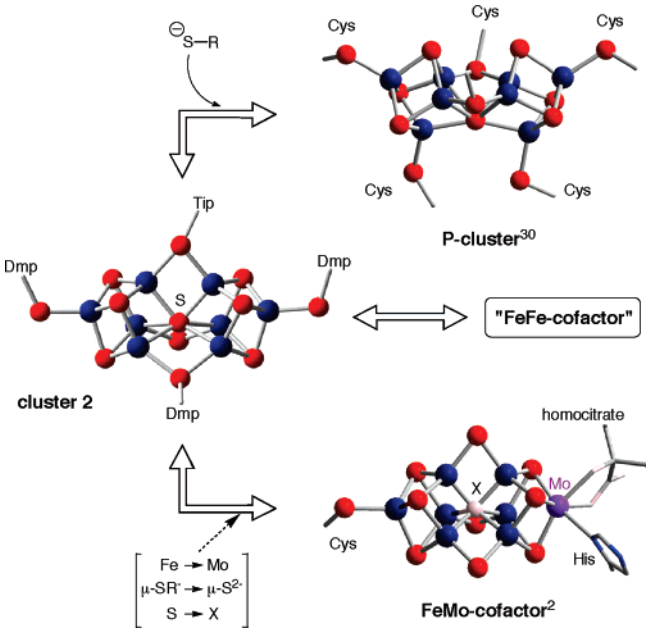

the samples were sealed into silver capsules in a glovebox. The EPR spectrum was recorded on a JEOL JES-FA200 spectrometer. Cyclic voltammogram was recorded in THF using glassy carbon as working electrode with 0.2 M $(Bu_4N)(PF_6)$ as supporting electrolyte. The potentials are reported in reference to Cp_2Fe/Cp_2Fe^+. The magnetic susceptibility was measured using a Quantum Design MPMS-XL SQUID-type magnetometer where the sample was sealed into a quartz tube. Iron(II) bisamide $Fe\{N(SiMe_3)_2\}_2$[7] and HSDmp (Dmp = 2,6-(mesityl)$_2C_6H_3$)[16a] were prepared according to the published procedures.

Synthesis of [(TipS)Fe(μ-SDmp)]$_2$ (1). To a hexane (40 mL) solution of 5.00 g (13.3 mmol) of $Fe\{N(SiMe_3)_2\}_2$ was slowly added a toluene (80 mL) solution of HSDmp (4.60 g,13.3 mmol). The color of the solution immediately turned from light green to yellow, indicating the formation of the known thiolate complex $Fe(SDmp)\{N(SiMe_3)_2\}$.[16a] After addition of a hexane (40 mL) solution of HSTip (3.14 g, 13.3 mmol), the resultant dark-red solution was stirred for 2 h at ambient temperature. All volatile materials were removed under reduced pressure, and the red residue was washed twice with 30 mL of hexane and filtered. A red crystalline powder of **1** (8.22 g, 97%) was obtained after drying under reduced pressure. Crystallization from toluene/hexane at room-temperature yielded single crystals suitable for crystallography. UV−vis (toluene, room temp): λ_{max} = 345 (sh, ϵ 6300), 427 (sh, ϵ 4000), 493 (sh, ϵ 2700) nm. Anal. Calcd for $C_{78}H_{96}Fe_2S_4$: C, 73.56; H, 7.60; S, 10.07. Found: C, 73.70; H, 7.28; S, 9.63.

Synthesis of [(DmpS)Fe$_4$S$_3$]$_2$(μ-SDmp)$_2$(μ-STip)(μ_6-S) (2). To a toluene (80 mL) solution of **1** (2.40 g, 1.88 mmol) was added a toluene (20 mL) solution of elemental sulfur S_8 (0.121 g, 0.472 mmol). After stirring for 4 days at ambient temperature, the solvent was removed under reduced pressure to give a black oily material. The residue was extracted with a mixture of toluene (10 mL) and hexamethyldisiloxane (20 mL), and the solution was centrifuged. Upon standing the extract at ambient temperature, black plates of **2**·$(C_6H_{18}OSi_2)_2(C_7H_8)_{1.5}$ (0.362 g, 28%) appeared. UV−vis (toluene, room temp): λ_{max} = 460 nm (ϵ 29000). Anal. Calcd for $C_{111}H_{123}Fe_8S_{12}$: C, 58.25; H, 5.42; S, 16.81. Found: C, 58.42; H, 5.69; S, 16.80. Cyclic voltammogram (2 mM in THF, room temp): $E_{1/2}$ = −0.74, −1.15, −2.00 V (vs Fc/Fc^+, all quasi-reversible). EPR (X-band, microwave 1.0 mW, 0.8 mM in frozen toluene, 10 K): g = 2.19, 2.07, 1.96.

Formation of 2 and [(TipS)Fe$_4$S$_3$]$_2$(μ-SDmp)$_2${(μ-N(SiMe$_3$)$_2$}(μ_6-S) (3) in the Reaction of Fe{N(SiMe$_3$)$_2$}$_2$/HSDmp/HSTip/S$_8$. To a

Table 3. Crystal Data and Structure Refinement for **1**−**3**

	1·(C_7H_8)	**2**·($C_6H_{18}OSi_2$)$_2$·(C_7H_8)$_{1.5}$	**3**
formula	$C_{85}H_{79}Fe_2S_4$	$C_{133.5}H_{149}O_2Fe_8S_{12}Si_4$	$C_{84}H_{114}NFe_8S_{11}Si_2$
fw	1340.49	2729.48	1993.44
crystal system	monoclinic	triclinic	monoclinic
temp (°C)	−100	−160	−100
space group	$P2_1/n$ (No. 14)	$P\bar{1}$ (No. 2)	$C2/c$ (No. 15)
a (Å)	12.378(2)	12.480(3)	28.225(6)
b (Å)	22.072(4)	15.646(4)	21.307(4)
c (Å)	13.876(2)	36.535(8)	22.393(5)
α (deg)		98.077(3)	
β (deg)	92.644(2)	89.789(2)	123.519(2)
γ (deg)		101.688(3)	
V (Å^3)	3787.1(11)	6915(3)	11227(4)
Z	2	2	4
D_{calcd} (g/cm$_3$)	1.175	1.311	1.179
μ(Mo Ka) (cm^{-1})	5.348	10.761	12.618
max 2θ (deg)	55.0	55.0	55.0
no. of data collected	44067	70448	45441
no. of unique data ith [$I > 2\sigma(I)$]	7020	23319	6479
no. of params refined	459	1581	521
R	0.0578	0.0647	0.0924
Rw	0.0838	0.1351	0.1458
GOF	1.035	1.004	1.011

[a] $R = \Sigma||F_o| - |F_c||/\Sigma|F_o|$. [b] $Rw = [\{\Sigma w(|F_o| - |F_c|)^2\}/\Sigma wF_o^2]^{1/2}$.

toluene (25 mL) solution of Fe{N(SiMe$_3$)$_2$}$_2$ (1.50 g, 3.98 mmol) was added a toluene (25 mL) solution of HSDmp (1.04 g, 2.99 mmol), a toluene (25 mL) solution of HSTip (1.18 g, 4.98 mmol), and a toluene (25 mL) solution of S_8 (0.112 g, 0.435 mmol). The resultant dark-brown solution was stirred for 2 days at ambient temperature. After removal of the solvent under reduced pressure, the black residue was washed with hexamethyldisiloxane (25 mL) and dried. The black solid was extracted with toluene (6 mL), and the extract was centrifuged to remove a small amount of insoluble materials. Upon standing the extract at −40 °C, black crystals (0.012 g) containing needles of **3** (major) and plates of **2** (minor) were grown. Several needle crystals of **3** were manually separated for the X-ray structure analysis. Since the separation of **2** and **3** in a larger scale was not possible, the mixed black crystals were subject to the EPR measurement. EPR (X-band, microwave 1.0 mW, 0.8 mM in frozen toluene, 15 K): major signals (cluster **3**), g = 2.13, 2.06, 1.93; minor signals (cluster **2**), g = 2.19, 2.07, 1.96; the intensity ratio, 10:3.

Formation of 2 and 3 in the Reaction of Fe$_3${N(SiMe$_3$)$_2$}$_2$(μ-STip)$_4$/HSDmp/ S$_8$. A 200 mL flask was charged with a toluene (40 mL) solution of Fe$_3${N(SiMe$_3$)$_2$}$_2$(μ-STip)$_4$[19] (2.00 g, 1.40 mmol). To this solution was added a toluene (30 mL) solution of HSDmp (0.969 g, 2.80 mmol) and a toluene (20 mL) solution of S_8 (0.118 g, 0.459 mmol). After stirring the solution for 2 days at ambient temperature, the solvent was removed under reduced pressure. The resultant black residue was washed with hexamethyldisiloxane (25 mL) and dried. The black solid was extracted with toluene (6 mL), and the extract was centrifuged to remove a small amount of insoluble materials. Upon standing the extract at −40 °C, black needles of **3** (major) and black plates of **2** (minor) grew (0.015 g). When the crystallization was carried out from Et$_2$O, crystals of **2** grew more readily than **3**.

X-ray Crystal Structure Determination. Crystallographic data are summarized in Table 3. Single crystals of **1**−**3** suitable for X-ray analysis were coated with oil (Immersion Oil, type B: Code 1248, Cargille Laboratories, Inc.) and mounted on a loop. Diffraction data were collected at −100 °C under a cold nitrogen stream on a Rigaku AFC8 equipped with a Rigaku Saturn 70 CCD/Micromax by using graphite-monochromated Mo Kα radiation. Six preliminary data frames were measured at 0.5° increments of ω, to assess the crystal quality and preliminary unit-cell parameters. The intensity images were measured at 0.5° intervals of ω. The frame data were integrated using the CrystalClear program package, and the data sets were corrected for absorption using a REQAB program. The calculations were performed with a TEXSAN program package. All structures were solved by a direct method, and refined by full-matrix least-squares. Cluster **2** was crystallized with hexamethyldisiloxane and toluene as crystal solvents, and an asymmetric unit contains 2 hexamethyldisiloxane molecules and 1.5 toluene molecules. One hexamethyldisiloxane appears as the superposition of two orientations with 1:1 occupancy factors. Toluene molecules were analyzed as one entire molecule and one-half molecule. The methyl group of half molecule was refined as 50% occupancy. Anisotropic refinement was applied to all non-hydrogen atoms except for the disordered isopropyl groups in **1**, the disordered hexamethyldisiloxane molecule in **2**·($C_6H_{18}OSi_2$)$_2$(C_7H_8)$_{1.5}$, and the para-isopropyl groups of STip in **3**. All hydrogen atoms were put at the calculated positions.

Acknowledgment. This research was financially supported by Grant-in-Aids for Scientific Research (No. 18GS0207 and 18064009) from the Ministry of Education, Culture, Sports, Science, and Technology, Japan. We thank W. Fujita, H. Yoshikawa, and K. Awaga (Nagoya University) for aiding us in the SQUID and EPR measurements.

Supporting Information Available: The cyclic voltammetry of **2**, the EPR spectrum of **3**, and a CIF file for **1**−**3**. This material is available free of charge via the Internet at http://pubs.acs.org.

JA072256B

(30) The structure of P-cluster was taken from 1QH8 (PDB). See reference 29b.